Premixed flames in narrow heated channels of circular cross-section: steady-state solutions, their linear stability analysis and dynamics.

Carmen Jiménez, Daniel Fernández-Galisteo and Vadim N. Kurdyumov
CIEMAT
Madrid, España

1 Introduction

Understanding the structure and dynamics of flames in narrow channels is important in the design of combustion devices such as, for example, small-scale recirculating super-adiabatic burners, which allow the burning of mixtures outside the flammability limits. These systems can present instabilities of various types, which can lead to undesirable consequences, such as uncontrolled flame behavior or even flame extinction.

One canonical configuration for studying flame dynamics in channels experimentally is an externally heated channel where only part of the channel wall is heated [1–6]. Heated channels have also received significant attention through numerical analysis [7-10] and it has been shown that when a fixed temperature profile is imposed at the wall an unexpectedly rich set of possible flame behaviors appears. From the experimental point of view, assigning a fixed temperature to the wall is probably not very realistic: when the flame contacts the channel wall, its temperature can hardly be constant, except may be in the case of a very high thermal conductivity wall. There are also obvious objective difficulties in measuring the temperature on the inner wall surface of the wall. For these reasons, the study via numerical simulations becomes fundamental for understanding the dynamics of flames in narrow heated channel.

In this work premixed flames in a narrow circular channel heated from the outside and subjected to a Poiseuille flow are investigated systematically for various Lewis numbers within the constant density model and using irreversible one-step Arrhenius kinetics. A global stability analysis of steady-state axisymmetric solutions is carried out, together with time-dependent direct numerical simulations, revealing the criteria for the emergence of oscillating flames with a cellular structure. The problem is also studied separately within the framework of the narrow-channel approximation. Finally, it is shown that chaotic flame dynamics may also appear.

2 Formulation

We consider a combustible mixture at initial temperature T_0 and fuel mass fraction Y_{F0} flowing in a

Correspondence to: vadim.k@ciemat.es

cylindrical channel with radius R. The total mass flow rate through the channel, m', is fixed. We use standard cylindrical coordinates with z', r' and φ' denoting the longitudinal, radial and angular coordinate, resp., and with t' denoting the time. We assume that the temperature profile of the outer surface of the wall can be controlled and is given by a profile $T_w(z')$.

We shall adopt a diffusive-thermal model, according to which the density of the mixture ρ, the heat capacity c_p, the thermal diffusivity D_T, and the molecular diffusivity D are all constants. Consequently, the flow field, unaffected by the combustion process, is given by the Poiseuille flow $u_z = 2U_0[1 - (r'/R)^2]$ and $u_r = u_\varphi = 0$, where $U_0 = m'/\pi\rho R^2$ is the mean flow velocity value. Moreover, we use a simplified kinetic model where the combustible mixture undergoes a chemical reaction modeled by a global irreversible step F + O → P + Q, where F, O and P denote the fuel, the oxidizer and the products, resp., and Q is the heat released per unit mass of fuel. Assuming that the mixture is lean in fuel, the oxidizer mass fraction remains nearly constant, and the reaction rate is $\Omega = B\rho^2 Y_F\, exp(-\mathcal{E}/\mathcal{R}T)$, where B is a pre-exponential factor containing Y_O and the molecular weights, $\mathcal{E}$ stands for the activation energy and $\mathcal{R}$ is the universal gas constant.

The burning velocity of the corresponding planar flame, S_L, and its thermal thickness defined as $\delta_T = D_T/S_L$ are used below to specify non-dimensional parameters. The non-dimensional temperature is defined as $\theta = (T - T_0)/(T_e - T_0)$, where $T_e = T_0 + Q\, Y_{F0}/c_p$ is the adiabatic temperature of the corresponding planar flame. Choosing δ_T and R as the reference length scales for z and r directions, resp., ${\delta_T}^2/D_T$ as the time scale, and Y_{F0} to normalize the fuel mass fraction, we have $(z, r) = (z'/\delta_T, r'/R), t = t'/\left({\delta_T}^2/D_T\right)$ and $Y = Y_F/Y_{F0}$, and the dimensionless equations written in the moving reference frame become:

$$\partial\theta/\partial t + 2\,m\,(1 - r^2)\;\partial\theta/\partial z \;=\; \partial^2\theta/\partial z^2 \;+\; 1/a^2\;\Delta_{r\varphi}\theta + \omega \qquad (1)$$

$$\partial Y/\partial t + 2\,m\,(1 - r^2)\;\partial Y/\partial z \;=\; 1/Le\left(\partial^2 Y/\partial z^2 \;+\; 1/a^2\;\Delta_{r\varphi}\theta\right) - \omega, \quad (2)$$

where $\Delta_{r\varphi} = \partial^2/\partial r^2 + r^{-1}\partial/\partial r + r^{-2}\,\partial^2/\partial\varphi^2$, $m = U_0/S_L$, $a = R/\delta_T$, $Le = D_T/D$ and $\omega = \beta^2/\left(2\,Le\,u_p^2\right) Y exp\{\beta(\theta - 1)/[1 + \gamma(\theta - 1)]\}$, with $\beta = \mathcal{E}\,(T_e - T_0)/\mathcal{R}T_e^2$ and $\gamma = (T_e - T_0)/T_e$.

These equations are to be solved subject to the following boundary conditions: The functions θ and Y are 2π-periodic functions of the angle φ. Because the radial temperature inside the wall is linear in r:

$$r = 1: \qquad \partial\theta/\partial r = -\frac{1}{2}a^2 b[\theta - \theta_w(z)], \;\; \partial Y/\partial r \;= 0,$$

where $b = 2\,(\lambda_w/\lambda)\,(\delta_T^2/Rh_w)$, with h_w the wall thickness and λ and λ_w the gas and wall thermal conductivity coefficients ($\lambda = \rho\, c_p D_T$).
For axisymmetric calculations ($\partial/\partial\varphi \equiv 0$)we impose symmetry conditions at the axis:

$$r = 0: \qquad \partial\theta/\partial r = \;\partial Y/\partial r \;= 0,$$

while for 3D calculations we use a procedure to ensure that the axis is free from singularities [11,12]. The temperature and fuel mass fraction take their prescribed values upstream:

$$Y = 1, \theta = 0 \text{ as } z \to -\infty,$$

while at the outlet we require:

$$\partial^2\theta/\partial z^2 \;=\; \partial^2 Y/\partial z^2 \;= 0 \text{ as } z \to -\infty.$$

We use the Heaviside step function to define the temperature profile on the outer wall:

$$\theta_w\,(z) = \;\theta_w\,H(z) \text{ where } H(z \le 0) = 0 \text{ and } H(z > 0) = 1.$$

3 Steady state and time dependent solutions

Steady and time-dependent computations are carried out in a finite domain, $z_{min} < z < z_{max}$, with typical values $z_{min} = -50$ and $z_{min} = 50$. The size of the domain is significantly varied in order to check independence of the results. The spatial derivatives are discretized on a uniform grid using second order, three-point central differences. The typical number of grid points is 2001 for 1D calculations, 1001 x 101 for 2D and 501 x 51 x 81 for 3D. The number of grid points was doubled in some cases without significant differences in results. Particular attention was paid to verifying that the outlet boundary did not affect the resulting numerical flame structure, in particular the flame position.

For unsteady calculations an explicit marching procedure was used with first order discretization in time. The typical time step was varied from $\tau = 10^{-4}$ to 10^{-5}. No significant differences were found in the results when τ was halved. In order to determine steady (but not necessary stable) 2D solutions, the steady version of Eqs. (1) and (2) was solved using a Gauss-Seidel method with over-relaxation.

In addition to unsteady calculations, we have also performed a linear stability analysis of the steady state solutions, following the method presented in [11,12].

4 Some selected results

Examples of results for steady-state axisymmetric calculations for different Lewis numbers are shown in Fig. 1. It can be seen that for $Le < 1$ the peak of the reaction zone is located at a distance from the channel axis. As the Lewis number increases, the reaction rate maximum moves towards the axis. At large Lewis, the transverse flame profile becomes almost planar near the axis (see the $Le = 4$ case).

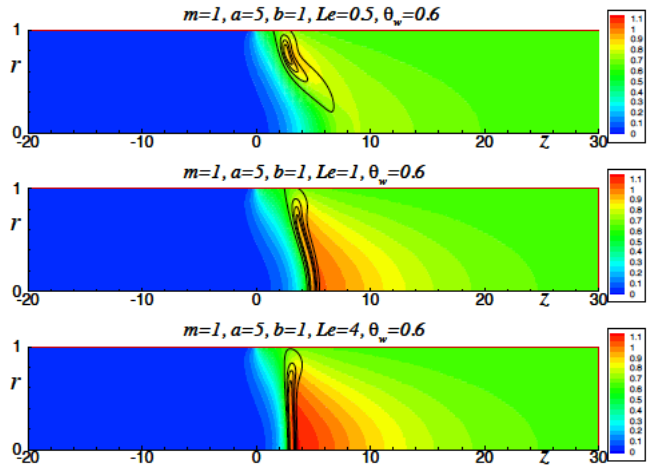

Figure 1: Examples of temperature (color plots) and reaction rates (black contours) for steady axisymmetric flames for several Le.

Figure 2 shows the dependencies of the real and imaginary parts of the main eigenvalue with the flow rate m for $Le = 1\ a = 5, b = 1$ and different modes with $n = 0,1,2,3$, obtained in the stability analysis. It can be seen that at low flow rates, the steady-state axisymmetric solution is stable. With a gradual increase in m the eigenvalue for $n = 0$ first becomes imaginary and then its real part passes to the right half-plane of the complex λ plane, that is, Hopf's bifurcation occurs. The value of the critical flow rate is plotted with vertical dash-dotted lines. A similar behavior is observed for modes $n > 0$. One can see that the real part of the eigenvalues with modes $n > 0$ also becomes positive with

increasing m, but modes with $n > 0$ are less unstable than the symmetric mode $n = 0$. It should also be noted that for sufficiently large m, the principal eigenvalues become purely real, as shown by the dashed lines in Fig. 2.

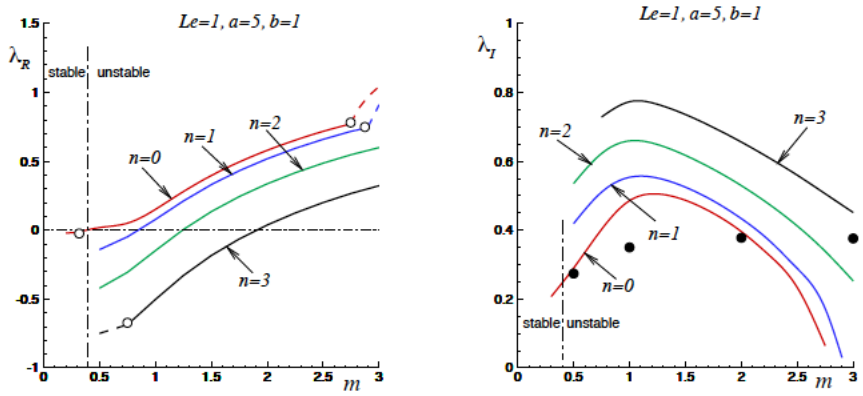

Figure 2: The real (left) and imaginary (right) parts of the main eigenvalue from stability analysis for the first four azimuthal wave numbers. The dashed segments on the left figure correspond to $\lambda_I = 0$ and the transition points from imaginary to real eigen-values are marked with open circles. The black circles in the right figure show the oscillation frequencies obtained in time-dependent simulations of Eqs. (1)-(2). The vertical dash-dotted line shows the stability boundary.

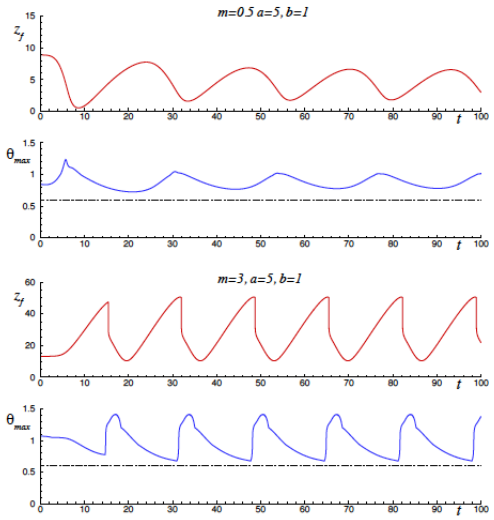

Figure 3: The flame position and maximum flame temperature results of time-dependent simulations of Eqs. (1)-(2). The measured oscillating frequencies are plotted with black circles in Fig. 2.

The time dependent evolution of the flame position and the maximum temperature reached in the channel obtained from Eqs. (1)-(2) are shown in Fig. 3 for two values of the flow rate, $m = 0.5$ and $m = 3$. In the case $m = 0.5$, the flow rate exceeds slightly the critical value above which the flame becomes unstable. Although the amplitude of the oscillations is noticeable, their frequency is close to the λ_I value obtained from the linear stability analysis (marked with a dark circle in Fig. 2). However, as the flow rate increases, a noticeable difference appears between the $\lambda_I$values obtained from the linear stability analysis and direct numerical simulations. This is especially evident for the case with $m = 3$, for which $\lambda_I = 0$ for the $n = 0$ mode, but, nevertheless, the flame experiences oscillations.

This case illustrates the repetitive extinction and ignition (FREI) regime when the flame is first carried away downstream from the beginning of the heating zone, and then re-ignition occurs, followed by a rapid upstream transition.

Figure 4 shows an example of the multiplicity of dynamic modes that take place at $Le = 0.5$. The plot shows a snapshot of the flame structure obtained in the case of oscillatory flame behavior. The right plot illustrates the purely cellular flame structure without oscillations. Interestingly, these two cases were obtained for the same parameter values. The appearance of chaotic dynamics at Lewis numbers greater than one is shown in Fig. 5 for $Le = 4$. The left figure shows the dependence of the flame position on time. On the right line there is a Poincaré map where the local maxima of the flame position are used to build it. It can be seen that the return map consists of several continuous segments, which indicates the chaotic behavior of the flame.

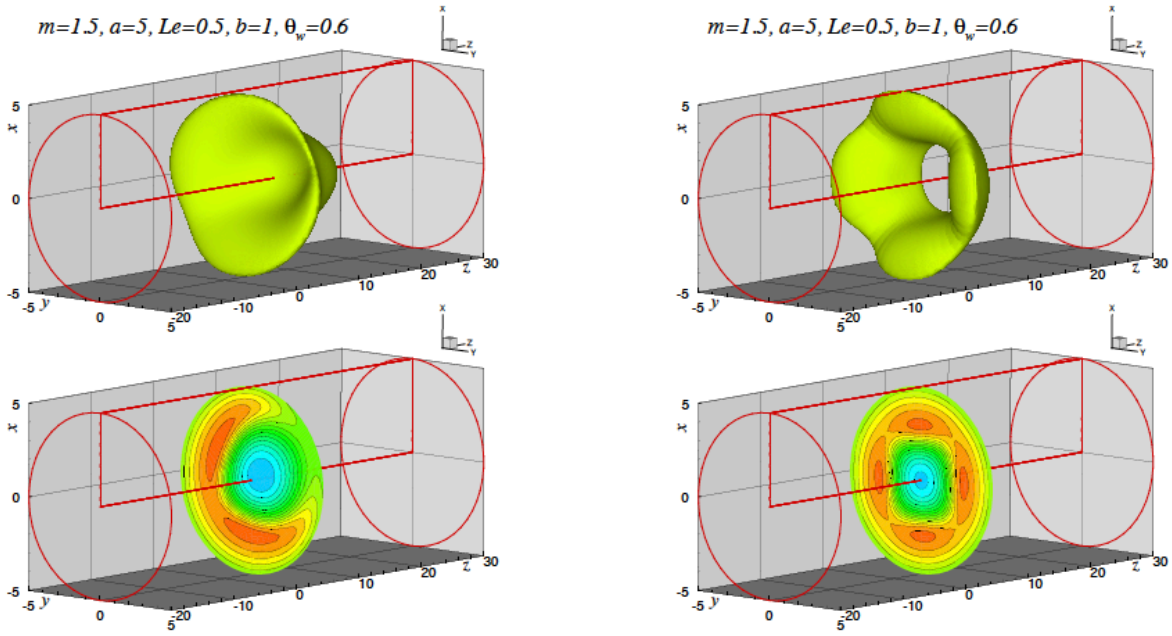

Figure 4: Example of a temperature iso-surface and the temperature distribution in section $z = z_f$. (Left) oscillatory dynamics, (right) time independent cellular structure.

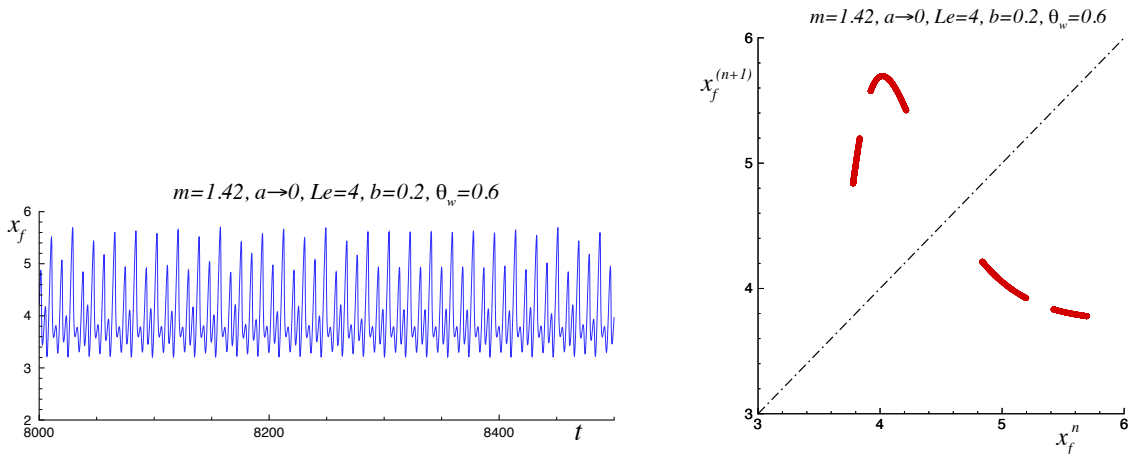

Figure 5: Example of the chaotic dynamics for a flame with $Le = 4$. The left plot shows the flame position versus time and the right plot shows the Poincaré map.

5 Conclusions

It is known that during local heating of the channel, additional effects associated with the transfer of heat in its wall have a significant effect on the flame. Analysis of the simplified model for narrow circular channels showed that despite its simplification, the behavior of the flame is extremely rich. The main goal of this study was to reveal the influence of the Lewis number on the flame dynamics. A global analysis of the stability of steady-state axisymmetric states has shown that when the Lewis number is less than one, a combination of oscillatory and cellular instability can take place. In this case, it was found that the multiplicity of modes for the same value of the parameters is also possible. For Lewis numbers greater than one, the appearance of chaotic flame dynamics is also shown for some values of the flow rate.

References

[1] K. Maruta, T. Kataoka, N.I. Kim, S. Minaev, R. Fursenko, Characteristics of combustion in a narrow channel with a temperature gradient, Proc. Combust. Int. 30 (2005) 2429-2436.
[2] M. Hori, H. Nakamura, T. Tezuka, S. Hasegawa, K. Maruta, Characteristics of n-heptane and toluene weak flames in a micro flow reactor with a controlled temperature profile, Proc. Combust. Int. 34 (2013) 3419-3426.
[3] T. Kamada, H. Nakamura, T. Tezuka, S. Hasegawa, K. Maruta, Study on combustion and ignition characteristics of natural gas components in a micro flow reactor with a controlled temperature profile, Combust. Flame 161 (2014) 37-48.
[4] H. Nakamura, S. Suzuki, T. Tezuka, S. Hasegawa, K. Maruta, Sooting limits and PAH formation of n-hexadecane and 2,2,4,4,6,8,8-heptamethylnonane in a micro flow reactor with a controlled temperature profile Proc. Combust. Int. 35 (2015) 3397-3404.
[5] S. Takahashi, H. Nakamura, T. Tezuka, S. Hasegawaa, K. Maruta, Multi-stage oxidation of a CH2F2/air mixture examined by weak flames in a micro flow reactor with a controlled temperature profile, Combust. Flame, 201 (2019) 140-147.
[6] A.K. Dubeya, T. Tezukaa, S. Hasegawaa, H. Nakamuraa, K. Maruta, Analysis of kinetic models for rich to ultra-rich premixed CH4/air weak flames using a micro flow reactor with a controlled temperature profile, Combust. Flame 206 (2019) 68-82.
[7] G. Pizza, C.E. Frouzakis, J. Mantzaras, A.G. Tomboulides, K. Boulouchos, Dynamics of premixed hydrogen/air flames in microchannels, Combust. Flame 152 (2008) 433-450.
[8] G. Pizza, C.E. Frouzakis, J. Mantzaras, A.G. Tomboulides, K. Boulouchos, Threedimensional simulations of premixed hydrogen/air flames in microtubes, J. Fluid Mech.m 658 (2010) 463491.
[9] V.N. Kurdyumov, G. Pizza, C.E. Frouzakis, J. Mantzaras, Dynamics of premixed flames in a narrow channel with a step-wise wall temperature, Combust. Flame 156 (2009) 2190- 2200.
[10] V.N. Kurdyumov, D. Fernández-Galisteo, C. Jiménez, Premixed flames in a narrow slot with a step-wise wall temperature: linear stability analysis and dynamics, Combust. Theor. Modell. 25 (2021) 1132-1157.
[11] V.N. Kurdyumov, C. Jiménez, V.V. Gubernov, A.V. Kolobov, Global stability analysis of gasless flames propagating in a cylindrical sample of energetic material: Influence of radiative heat losses, Combust. Flame 162 (2015) 1996-2005.
[12] V.N. Kurdyumov, C. Jiménez, Structure and stability of premixed flames propagating in narrow channels of circular cross-section: Non-axisymmetric, pulsating and rotating flames, Combust. Flame 167 (2016) 149-163.